Construction and Building Materials 183 (2018) 32–45

Contents lists available at ScienceDirect

Construction and Building Materials

journal homepage: www.elsevier.com/locate/conbuildmat

Experimental and analytical analysis of the effect of fibre treatment on the thermomechanical behaviour of continuous carbon textile subjected to simultaneous elevated temperature and uniaxial tensile loadings

Manh Tien Tran [a,b], Xuan Hong Vu [a,*], Emmanuel Ferrier [a]

[a] University of Lyon, University Claude BERNARD Lyon 1, Laboratory of Composite Materials for Construction (LMC2), 82 bd Niels Bohr, F-69622 Villeurbanne, France
[b] Hanoi University of Mining and Geology (HUMG), n°18, Pho Vien street, Duc Thang ward, Bac Tu Liem district, Hanoi City, Viet Nam

ARTICLE INFO

Article history:
Received 10 February 2018
Received in revised form 6 June 2018
Accepted 14 June 2018

Keywords:
Continuous carbon textile
Fibre treatment
Elevated temperature
Thermomechanical behaviour
Stress–strain curve

ABSTRACT

In the case of fire, the carrying capacity of the textile-reinforced-concrete (TRC) depends greatly on the thermomechanical behaviour of the reinforcement textile at elevated temperatures. Carbon textiles are manufactured in industry as commercial products for application in TRC. The treatment of carbon fibres by products of different natures in the manufacturing chain also influences the thermomechanical behaviour and mechanical property evolution as a function of temperature. This paper presents an experimental study on the tensile behaviour of three different continuous carbon textiles subjected to simultaneous mechanical loading and elevated temperatures (varying from 25 °C to 600 °C). The results on three carbon textiles are compared to understand the effect of fibre treatment on the thermomechanical behaviour of carbon textile. The experimental results are used to calibrate a prediction analytical model (Mouritz and Gibson), which can be applied to the thermomechanical estimation of carbon textile under different temperature and mechanical conditions.

1. Introduction

In the field of civil engineering, the construction industry is in need of a new shift. One way to face this need is exploring the use of alternative building materials. Composite materials are often used to repair and/or strengthen the structural elements (slab, beam, column...) of old civil engineering works. These composite materials can also be used as supporting elements in new structures [1,2]. Over the past two decades, textile-reinforced concrete (TRC) composite material (carbon fibre, glass fibre, aramid fibre, etc.) has become increasingly widely used to repair or strengthen structures [2–4]. The textile in composite material plays a very important role in the carrying capacity and stiffness of composite materials. Among textiles used, carbon textile provides better supported load capacities, high strength, and high Young's modulus to traction [5,6]. This is the main reason for the manufacture of carbon textiles as commercial products for application in TRC composite to repair and/or strengthen structural elements of existing construction works (bridge, building, tunnel, etc.) [7]. Following paragraphs present the previous studies that have focused on TRC and FRP behaviours under fire or different temperatures. The objective of this study ends the introduction of this paper.

1.1. TRC behaviour under fire or different temperatures

Several studies have been conducted at ambient temperature on the tensile or bending behaviour of textile-reinforced concretes [8–10]. In the case of fire in a civil engineering structure strengthened by carbon-textile-reinforced-concrete composite (bridge, building, tunnel, etc.), composite material is simultaneously subjected to mechanical loading and elevated temperatures (potentially up to 1200 °C). Until now, studies on the fire behaviour of TRC material have been rare because of experimental difficulties linked to fire tests. Some fire tests have been performed on thin, high-performance concrete plates, reinforced with basalt fibre-reinforced polymer mesh [11], on carbon fibre-reinforced, fine-grained concrete [12], and on I-shaped beams, reinforced with glass-fibre and carbon-fibre mesh grids [13,14]. A few studies have been investigated on the residual mechanical behaviour of TRC after exposure to elevated temperatures [15–18]. Few studies have been conducted on the thermo-mechanical behaviour of TRC. The thermo-mechanical behaviour of a carbon fabric-reinforced cementitious matrix composite (at temperatures ranging from 20 °C to 120 °C) [19] and that of a basalt fabric-reinforced

* Corresponding author.
E-mail addresses: Xuan-Hong.Vu@univ-lyon1.fr (X.H. Vu), emmanuel.ferrier@univ-lyon1.fr (E. Ferrier).

https://doi.org/10.1016/j.conbuildmat.2018.06.114
0950-0618/

cementitious matrix composite (at temperatures ranging from 20 °C to 400 °C) [20] have been performed. The effects of simultaneous mechanical loading and elevated temperature (for temperatures ranging from 20 °C to 400 °C) on the behaviour of the glass TRC have been experimentally studied [21]. Few researchers have focused on behaviour of TRM versus FRP composite as strengthening materials at high temperatures that were evaluated in shear, bond and flexure [22–24]. The thermomechanical behaviour of the TRC composite depends on several factors such as the nature and configuration of the textile reinforcements, the reinforcement ratio, the nature of the matrix, and the pre-impregnation of the textiles by different products. Among these factors, the load capacity of the carbon textile at elevated temperatures strongly influences the thermomechanical behaviour of the TRC composite because the TRC matrix is strongly damaged under elevated temperature conditions. At ambient and low temperature levels, the tensile uniaxial behaviour of TRC shows a stress–strain curve with three distinguishable phases corresponding to the TRC behaviour before the matrix cracking (first phase), during the matrix cracking (second phase), and during the post-cracking of the matrix (third phase) [20,21]. At ambient temperature and low temperature level, during the third phase of the stress–strain curve of TRC, the concrete matrix is completely cracked, so there is the only work of continuous textile before the rupture of the composite. Understanding the thermomechanical behaviour of the continuous textile reinforcement makes it possible to estimate the thermomechanical behaviour of TRC. This justifies the need to study the thermomechanical behaviour of the continuous reinforcement textile.

1.2. FRP behaviour under fire or different temperatures

In the literature, there were few studies on the effect of fire or elevated temperatures on the behaviour of reinforcement textiles or continuous fibres reinforced polymer (FRP) products to strengthen structures. In their recent works, Rambo et al. [20] carried out tests on samples of basalt textiles in a preheating–cooling regime with five temperature levels (25 °C, 75 °C, 150 °C, 200 °C, and 400 °C). They also explained the contribution of a styrene-acrylic latex coating to the residual behaviour of basalt textile. The fire behaviour of a carbon/epoxy laminate composite for aircrafts [25] and the fire stability of the carbon fibre-reinforced polymer (CFRP) shell [26] have been studied. Boyd et al. [27], Bausano et al. [28], Feih et al. [29] and Mouritz et al. [30] have performed experimental and numerical studies on polymer composite (glass fibre, carbon fibre) under fire condition or heat flux conditions. The tensile performance of the basalt fibe-epoxy laminate [31] and the carbon-epoxy laminate [32] under combined one-sided radiant heating and axial tensile loading have been performed. Some studies have focused on elevated temperature behaviour of CFPR [33–38]. Most of these studies showed the evolution of the mechanical properties of carbon fibres or CFRP according to temperature. In the work of Green et al. [34], the carbon fibres were practically unaffected by an elevated temperature up to 1000 °C, whereas the CFRP composite lost most of its resistance at 600 °C. Wang et al. [37] presented their study on "preheated-cooled" CFRP composite specimens for residual behaviour at temperature levels ranging from 22 °C to 706 °C. Yu and Kodur [38] tested CFRP rod or strip specimens at elevated temperatures. Nguyen et al. [39] conducted the characterization of pultruded carbon fibre reinforced polymer (P-CFRP) under two elevated temperature-mechanical load cases: residual and thermo-mechanical regimes. All works also showed a reduction in tensile strength and rigidity of CFRP composite with increasing temperature. Otherwise, the fire/heat and mechanical performance of the glass-reinforced epoxy composites (glass FRP) has been performed [40–42]. The microstructure and mechanical properties of carbon microfiber reinforced geopolymers at elevated temperatures have been experimentally studied [43]. The thermomechanical properties and bond characteristics of different fiber (carbon, basalt, glass) reinforced polymer rebars at elevated temperatures (from 20 °C to 500 °C) have been experimentally investigated [44]. The mechanical properties of CFRP laminates at elevated temperatures and freeze–thaw cycling (for temperatures ranging from -50 °C to 150 °C) have been studied [45]. The thermomechanical properties of glass fibre reinforced GFRP reinforcing bars at high temperatures (ranging from 25 °C to 500 °C) have been experimentally identified [46]. The cyclic thermal effects (for temperatures ranging from 20 °C to 200 °C) on the mechanical behaviour of CFRP laminate [47] or FRP [48,49] have been investigated.

1.3. Objective of this study

To the best of the authors' knowledge, no results are available concerning experimental tests with simultaneous mechanical and elevated temperature loadings carried out on continuous carbon textile specimens. There are also no results regarding the effect of fibre treatment on the thermomechanical behaviour of continuous carbon textile at elevated temperatures. With the synthesis of previous research works, some scientific questions can be asked: Is it possible to experimentally obtain the "stress–strain" relation of continuous carbon textile when it is subjected to combined thermal and mechanical loadings (at elevated temperatures)? What is the thermomechanical behaviour of continuous carbon textile at elevated temperatures? What is effect of fibre treatment on the thermomechanical behaviour of continuous carbon textile (evolution of mechanical properties according to temperature, modes of rupture)? What analytical model allows the mechanical property evolution of continuous carbon textile according to temperature to be predicted? The aim of this work is to contribute in answering these questions. This work will also provide the scientific community with experimental data concerning the thermomechanical behaviour of three continuous carbon textiles (with different fibre treatments).

This paper presents an experimental study on the tensile behaviour of three different continuous carbon textiles subjected to simultaneous mechanical and elevated temperature loadings. By using an innovative thermomechanical machine (TM20kN-1200C), direct tensile tests on specimens of three continuous carbon textiles (with fibres treated by different products) were carried out at different temperature levels varying from 25 °C to 600 °C. The results on three carbon textiles were compared to understand the effect of fibre treatment on the thermomechanical behaviour of carbon textile. In this article, an analytical model will be chosen and calibrated to predict the effect of temperature on the thermomechanical behaviour of carbon textiles. In the following sections of this paper, experimental work including the use of equipment, test specimens and test procedure are presented (Section 2). The experimental results will then be presented, analysed and discussed (Section 3). The analytical modelling work will then be shown (Section 4). This paper ends with a presentation of main conclusions and future works.

2. Experimental work

This section presents the used equipment, used materials, specimen production and preparation, summary of specimens, and tests and test procedure.

2.1. Used equipment

In this section, the test machine, the specimen strain measurement, and the temperature instruments will be presented in detail. This section shows how to generate simultaneous action of mechanical loading and elevated temperature and how to measure the strain of the test specimens in the thermomechanical condition.

2.1.1. Thermomechanical test setup

The experimental study of carbon textile test specimens was carried out using a universal traction machine (TM20kN – 1200 °C) at the LMC2 Laboratory (Lyon, France) (Fig. 1). This machine has a mechanical capacity of 20 kN and is equipped with a cylindrical furnace that can generate temperature loadings of specimens potentially up to 1200 °C. Fig. 1 shows the configuration of the used thermomechanical machine. The used furnace (Fig. 1b,c) has

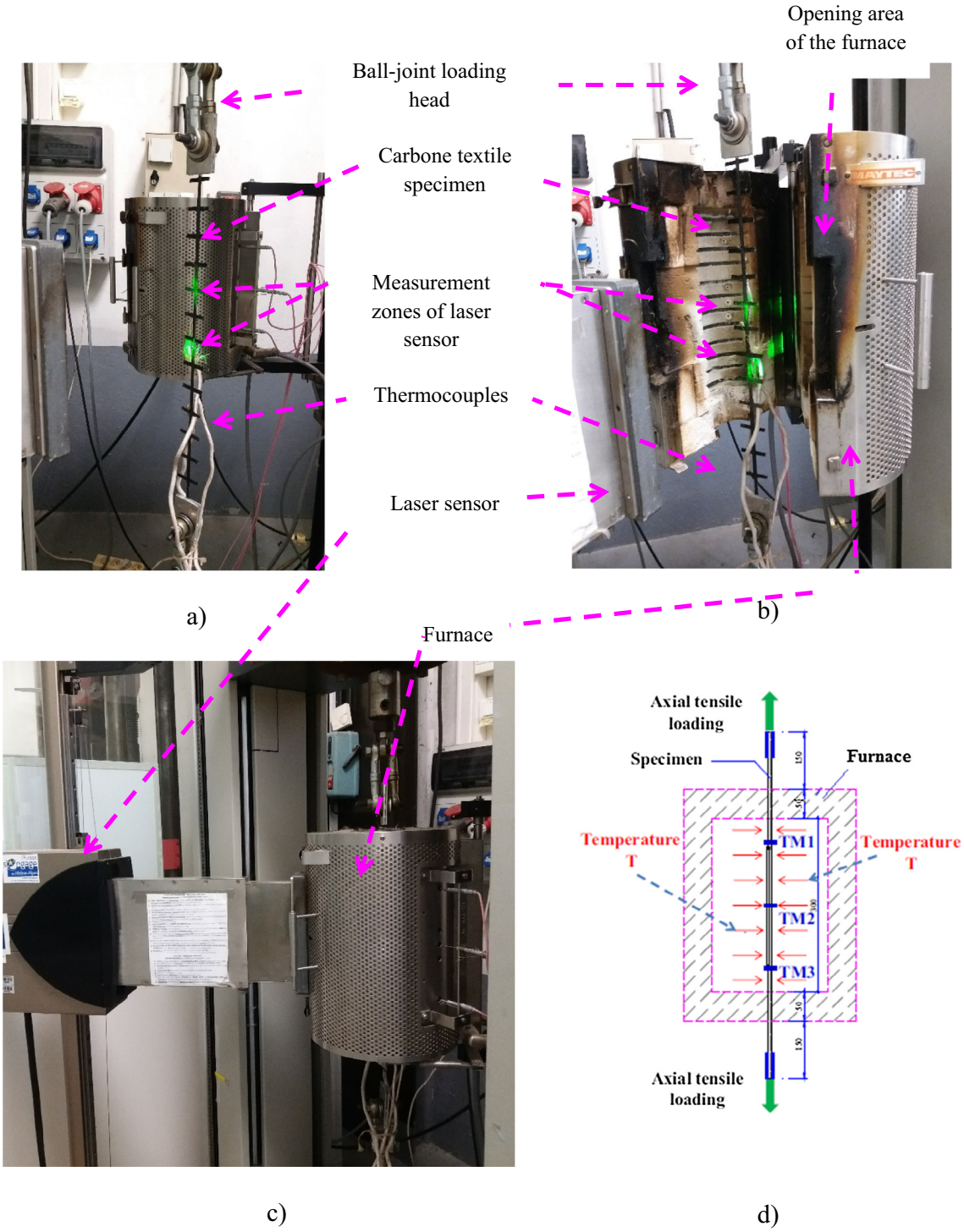

Fig. 1. Thermo-mechanical test setup (TM20kN-1200C); (a): Test at 25 °C carried out on carbon textile specimen; (b) Setup of the furnace around the test specimen; (c) Overview of the test setup; (d) Scheme of the direct tensile test at a temperature T: furnace, specimen, and three thermocouples (TM1, TM2, TM3).

a height of 40 cm, an internal diameter of 10 cm, and an external diameter of 27.5 cm. The maximum heating rate of this furnace is 30 °C/min. The temperatures in the furnace are controlled by integrated thermocouples. This experimental device makes it possible to apply simultaneous tensile mechanical and elevated temperature loadings on a sample. The laser sensor equipped on the machine is used to measure the longitudinal deformation of test specimens at elevated temperatures (non-contact measurement method).

2.1.2. Laser sensor

As presented in Section 2.1.1, the laser sensor (Fig. 1a,b,c) is used to measure the strain of test specimens in the test campaign. It is a new measurement method that takes non-contact measurements of axial strains on different materials. The measurement principle of this method is explained by the description of the laser sensor system. A laser bobbin is deflected by a rotating, multi-faced mirror so that it continuously scans the specimen lengthwise. A cylindrical lens between the mirror and specimen ensures a parallel bobbin over the entire measurement path (see Fig. 2). The light reflected from the specimen surface is guided via a lens system to a photodiode that generates an analogue measurement system that is dependent upon the brightness. The measurement marks are detected by their differences in brightness to that of the specimen.

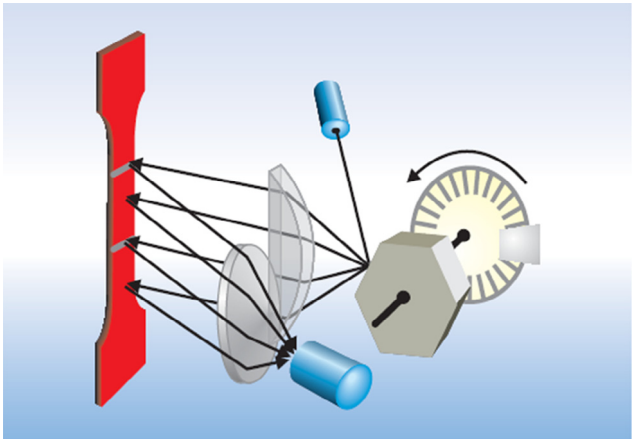

Fig. 2. Measurement principle of the laser sensor.

There are the difficulties for contact strain measurement method: the existence of a small furnace around the test specimen, the thinness of the test specimen of carbon textile, the high temperature in the furnace. With the non-contact measurement method by the laser sensor, the axial strain of the carbon textile specimen is determined by the ratio of the relative displacement of two laser bobbins and their initial distance. This method of measurement has been used, developed, and validated in previous works and has given good results for different composite materials [21,39].

2.2. Specimens

This section first shows continuous carbon textiles studied in this experiment. It then presents the preparation of carbon textile specimens for thermomechanical tests.

2.2.1. Studied carbon textiles

The continuous carbon textiles used in this experiment are industrial products that were manufactured in a factory. The three carbon textiles were coated with different treatment products in nature. They were manufactured in grid form with different grid geometries. The properties of the three studied carbon textiles are summarized in Table 1. The images and geometries of the studied carbon textile grids are shown in Fig. 3.

The technical details of the used carbon textiles (GC1, GC2, GC3) are shown below:

– GC1 carbon textile (Fig. 3a): This textile was produced with an epoxy resin coating. The geometry of the grid in the longitudinal and transverse directions is 46 mm × 41 mm (see Fig. 3). The cross section of a wire (the warp as well as the weft) is 1.85 mm^2. This carbon textile has good characteristics: non-corrosion, requirement of a less concrete cover. This characteristic leads to lighter structures, ease of handling and use, high strength and tensile modulus, and a remarkable mechanical bond with concrete.

Table 1
Properties of three studied carbon textiles [GC1(or 2, 3)]; GC: grid of carbon textile (supplier's data).

Properties	GC1	GC2	GC3
Density (g/cm^3)	3.43	1.79	1.89
Grid geometry (longitudinal × transverse spacing) (mm × mm)	46 × 41	17 × 17	33 × 33
Type of coating	epoxy resin	amorphous silica	epoxy resin
Cross-sectional area of one individual strand	1.85 mm^2	1.795 mm^2	1.80 mm^2

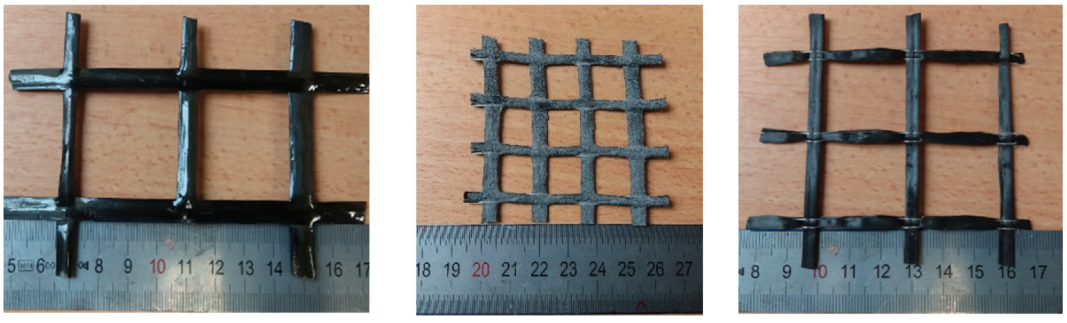

(a) GC1 carbon textile (b) GC2 carbon textile (c) GC3 carbon textile

Fig. 3. Images of three carbon textiles (GC1, GC2, GC3) used in the experimental study.

– GC2 carbon textile (Fig. 3b): This textile was made of bi-directional, high-strength carbon fibre mesh for low-thickness structural reinforcements. This textile also has advantages such as very high tensile strength, good resistance to corrosion, low mass per unit area, simple and flexible application (also on the underside of slabs), coating with amorphous silica for perfect adhesion with concrete aggregates, high resistance to heat, and low reinforcement thickness. The geometry of the grid in the longitudinal and transverse directions is 17 mm × 17 mm (see Fig. 3), and the warp and weft are formed by approximately 3200 monofilaments (longitudinal 2 × 1600 tex/strand and transverse 1 × 3200 tex/strand).
– GC3 carbon textile (Fig. 3c): This textile is a similar commercial product to the first textile, but the rate of epoxy resin for the treatment is very low. The spacing of the longitudinal and transverse yarn (chain and weft) is 33 mm × 33 mm (see Fig. 3c).

2.2.2. Specimen preparation

The test specimens in this experimental study were prepared by hand in the laboratory. First, the carbon textiles are unrolled on a plane, and they were flattened for one day. Afterwards, a longitudinal yarn (the warp) of the textile was cut to obtain carbon textile samples of 750 mm in length. For good transmission of the mechanical force to the textile specimens, two aluminium plates (dimension of 60 m × 140 mm) were bonded to each end of the specimens by the epoxy adhesive (Eponal 380) (see Fig. 4a). Sometimes, it is necessary to use bolts to better reinforce two aluminium plates. These bolts allowed better adhesion between the textile and aluminium plates (see Fig. 4b). During the preparation of the carbon textile specimens, it is necessary to cover the technical details that may affect the experimental results. Some such technical details include placing the test specimens in the same plane and avoiding torsional force in the samples. All professional preparation procedures give a better result after the test. The specimens were stored at room temperature for 7 days for curing of the adhesive (see Fig. 4a). Each carbon textile specimen was then referenced and ready for the tests at different temperatures.

2.3. Summary of specimens and tests

Table 2 shows the list of the specimens and the tests carried out. There were 42 tests carried out on the specimens of three carbon textiles at different temperature levels varying from 25 °C to 600 °C. For some tests (1 for GC1 at 600 °C, 2 for GC2 at 600 °C and 3 for GC3 at 500–600 °C), the carbon textile specimens were broken at high temperature during the thermal exposure phase (at the target temperature) before the thermomechanical loading phase. The procedure of the tests carried out is presented in Section 2.4.

2.4. Test procedure

The loading chosen for the tests carried out on the carbon textile specimens (Fig. 5) consists of the following three phases:

– The first test phase (Fig. 5) consists of increasing the temperature around the sample to the desired temperature level. For technical reasons, the furnace requires approximately 30 min to reach the target temperature (T_{target}). This duration can ensure good operation of the furnace. After 30 min, the temperature is homogenized around the sample placed in the furnace.

(a) Embracing for specimens (b) Carbon textile samples ready for test

Fig. 4. Preparation of samples.

Table 2
List of tests conducted on the specimens of three carbon textiles.

Designation of the specimen	Dimensions of the specimen [cross section, S (mm^2) length, l (mm)]	Temperature (°C)	Exposure duration	Number of tests
GC1-25-a,b,c	S = 1.85 (mm^2); l = 425 (mm)	25	–	3
GC1-200-a,b,c		200	1 h	3
GC1-400-a,b,c		400	1 h	3
GC1-500-a,b,c		500	1 h	3
GC1-600-a,b		600	1 h	2
GC2-25-a,b,c	S = 1.795 (mm^2); l = 420 (mm)	25	–	3
GC2-200-a,b,c		200	1 h	3
GC2-400-a,b,c		400	1 h	3
GC2-500-a,b,c		500	1 h	3
GC2-600-a,b		600	1 h	2
GC3-25-a,b,c	S = 1.80 (mm^2); l = 425 (mm)	25	–	3
GC3-200-a,b,c		200	1 h	3
GC3-400-a,b,c		400	1 h	3
GC3-500-a,b,c		500	1 h	3
GC3-600-a,b		600	1 h	2
Total of tests				42

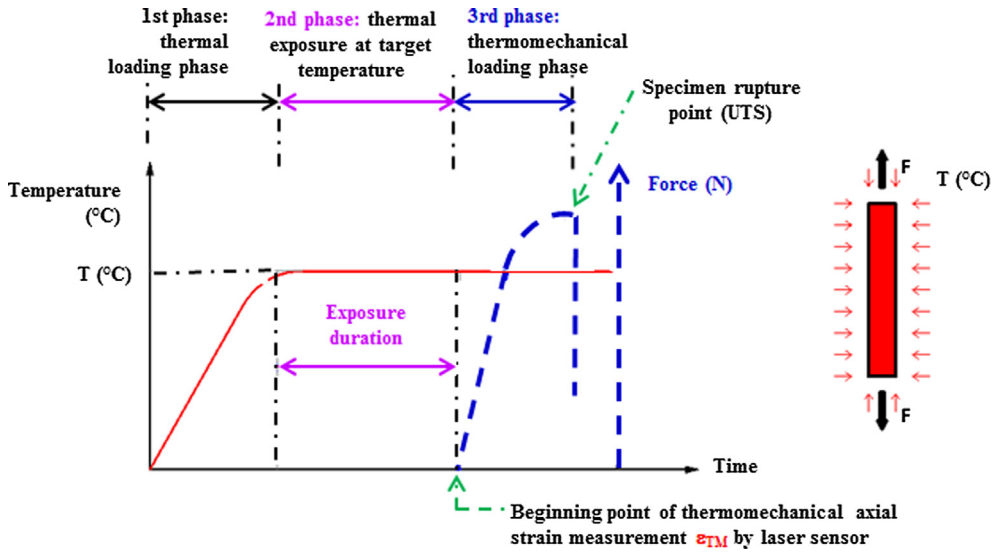

Fig. 5. Loading path of thermomechanical tests carried out on specimens of three carbon textiles [21].

The rate of temperature increase varies from 6 °C/min to 20 °C/min depending on the target temperature (from 200 °C to 600 °C) of the test.

- The second test phase (Fig. 5) consists of maintaining the target temperature (T_{target}) for a period of 1 h to homogenize the temperature around the textile specimens (see Fig. 5). The laser sensor cannot measure the axial deformation of textile samples due to technological difficulties during the temperature increase from 25 °C to T_{target} (first phase). Therefore, it is deactivated in the first and second phases because of technological difficulties.
- The third test phase (Fig. 5) consists of applying the mechanical quasi-static load monotonically to the specimen until failure. In this phase, the laser sensor is activated to measure the axial strain of the sample from the beginning of the third phase until specimen failure. The stress of the specimen corresponding to the failure point is quantified as the ultimate stress of the carbon textile (or σ_{UTS}). The axial strain of the specimen corresponding to the failure point is quantified as the maximum axial thermomechanical deformation of the textile, or $\varepsilon_{TM,\ UTS}$ (see Fig. 5).

Fig. 5 shows the thermomechanical test procedure on the test specimens of carbon textiles with three phases. After the test, all data, including temperatures, mechanical load, and specimen axial thermomechanical strain or traverse movement, are recorded at least twice per second and can then be exported in the form of datasheets for results analysis.

3. Results

This section presents the results of thermomechanical tensile tests and evolution of the thermomechanical properties as a function of temperature.

3.1. Results of thermomechanical tensile tests

This section shows the results of the thermomechanical tensile tests carried out on three studied carbon textiles and the evolution of the thermomechanical properties of carbon textiles as a function of temperature.

3.1.1. Results of the GC1 textile specimens

Fig. 6 shows the experimental results carried out on the GC1 carbon textile samples; they are the "stress–strain" curves at different temperatures ranging from 25 °C to 600 °C. In this figure, for each temperature level, there is an average "stress–thermo mechanical strain" curve that was selected among the curves obtained from the tests carried out on the GC1 textile specimens under the same thermomechanical condition. The GC1 textile samples exposed for 1 h at elevated temperatures gave an almost linear behaviour up to the failure of the test specimen (see Fig. 6). The ultimate strength of the GC1 carbon textile at 25 °C is 2616.6 MPa, whereas this value at elevated temperatures decreases progressively as a function of temperature. At 600 °C, the GC1 carbon textile gave an ultimate strength of 204.9 MPa (see Table 3) corresponding to a 92.8% reduction of this value at ambient temperature. Regarding Young's modulus of the GC1 carbon textile, it can be seen in Fig. 6 that the slope of the "stress–thermomechanical strain" curves of the GC1 textile thermomechanical behaviour also decreases when the temperature increases. At room temperature, Young's modulus of GC1 carbon textile determined by two points corresponding to the deformation of 0.0005 and 0.0025 was 256.2 GPa, whereas the thermomechanical test at 600 °C gave a very low Young's modulus value of 29.5 GPa (see Table 3) corresponding to 11.5% of its Young's modulus at 25 °C.

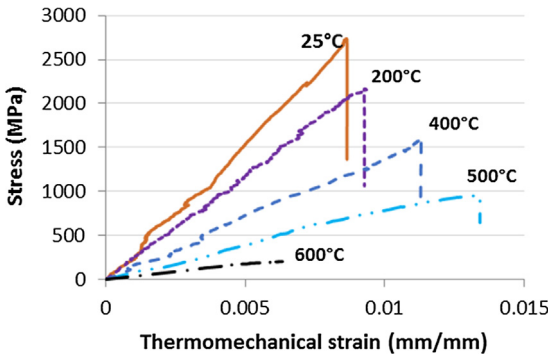

Fig. 6. Thermomechanical behaviour of the GC1 carbon textile: stress–thermomechanical strain relationship at different temperatures.

Table 3
Results of the direct tensile tests performed on the GC1 carbon textile.

Sample's ID	T °C	Temperature increase rate (°C/min)	Ultimate stress (MPa)	Average stress (MPa)	Standard deviation (MPa)	Young's modulus (GPa)	Average modulus (GPa)	Standard deviation (GPa)
GC1 – 25 °C - a	25	0	2733.6	2616.6	124.9	296.8	256.2	39.7
GC1 – 25 °C - b			2485.0			254.4		
GC1 – 25 °C - c			2631.1			217.5		
GC1 – 200 °C - a	200	6.70	2347.6	2169.5	175.5	171.7	201.6	29.0
GC1 – 200 °C - b			1996.6			203.4		
GC1 – 200 °C - c			2164.3			229.7		
GC1 – 400 °C - a	400	12.52	1652.2	1652.2	40.5	126.3	138.8	23.4
GC1 – 400 °C - b			1692.7			165.8		
GC1 – 400 °C - c			1611.7			124.2		
GC1 – 500 °C - a	500	16.00	960.7	795.7	145.4	79.3	77.6	4.5
GC1 – 500 °C - b			739.9			80.9		
GC1 – 500 °C - c			686.5			72.5		
GC1 – 600 °C - a	600	17.95	204.9	204.9	0	29.5	29.5	0
GC1 – 600 °C - b			NA			NA		

Table 3 presents the other values in the results of thermomechanical tests on the GC1 carbon textile specimens at different temperature levels varying from 25 °C to 600 °C. It also gives the average values and the standard deviation values of the mechanical properties of GC1 carbon textile as a function of the temperature. The maximum value of the standard deviation on the ultimate stress data of the GC1 carbon textile was 175.5 MPa at 200 °C, corresponding to 8.1% of its average ultimate stress at this temperature. The maximum value of the standard deviation on the Young's modulus data of the GC1 carbon textile was 39.7 GPa at 25 °C, corresponding to 15.5% of its average Young's modulus at room temperature. The standard deviation values demonstrate the convergence of these experimental results.

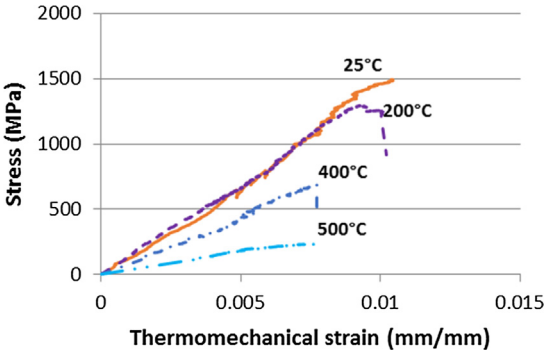

Fig. 7. Thermomechanical behaviour of the GC2 carbon textile: stress–thermomechanical strain relationship at different temperatures.

3.1.2. Results of the GC2 textile specimens

Fig. 7 shows the "stress–thermomechanical strain" relationships of the thermomechanical behaviour of GC2 carbon textile for temperature levels ranging from 25 °C to 500 °C. In this figure, for each temperature level, there is an average "stress–thermomechanical strain" curve that was selected among the curves obtained from the direct tensile tests in the same thermomechanical condition on the GC2 textile specimens. In Fig. 7, it can be seen that the GC2 carbon textile typically gives a quasi-linear behaviour up to failure. The results obtained on the GC2 textile specimens had the same tendency in the thermomechanical property evolution (ultimate strength, Young's modulus) depending on the temperature as the GC1 carbon textile. There is a great reduction in the ultimate strength and Young's modulus from the temperature of 400 °C (approximately 50%), which will be explained and discussed in Section 3.2. As results, the GC2 carbon textile provided ultimate strength ranging from 1311.5 MPa (average value at 25 °C) to 308.1 MPa (average value at 500 °C) (see Table 4). The two tests at 600 °C did not give the data on the stress and the longitudinal

Table 4
Results of the direct tensile tests performed on the GC2 carbon textile.

Sample's ID	T °C	Temperature increase rate (°C/min)	Ultimate stress (MPa)	Average stress (MPa)	Standard deviation (MPa)	Young's modulus (GPa)	Average modulus (GPa)	Standard deviation (GPa)
GC2 – 25 °C - a	25	0	1211.4	1311.5	158.3	150.4	143.8	7.2
GC2 – 25 °C - b			1494.0			136.1		
GC2 – 25 °C - c			1229. 2			145.0		
GC2 – 200 °C - a	200	6.91	1296.5	1152.5	204.9	130.4	138.6	14.0
GC2 – 200 °C - b			918.0			154.8		
GC2 – 200 °C - c			1243.1			130.6		
GC2 – 400 °C - a	400	13.11	689.9	708.8	71.8	87.2	107.1	18.6
GC2 – 400 °C - b			788.1			124.0		
GC2 – 400 °C - b			648.2			110.4		
GC2 – 500 °C - a	500	17.27	235.4	308.1	67.8	34.5	39.7	9.5
GC2 – 500 °C - b			319.3			33.9		
GC2 – 500 °C - c			367.6			50.7		
GC2 – 600 °C - a	600	20.86	NA	–	–	NA	–	–
GC2 – 600 °C - b			NA			NA		

NA: not available.

deformation because the test specimens were broken during the temperature exposure time (second phase). Regarding Young's modulus, the GC2 carbon textile had progressively decreasing stiffness as a function of temperature. This value was 143.8 GPa (average value) at 25 °C and 39.7 GPa (average value) at 500 °C (see Table 4). Table 4 shows the experimental results for all GC2 textile samples. As shown in Table 4, the tests carried out at 500 °C yielded sensitive results, which caused the high standard deviation value of the ultimate strength data (22.0% relative to the average value).

In the GC2 carbon textile results, the maximum standard deviation value of the ultimate strength data was 204.9 MPa at 200 °C, corresponding to a value of 17.8% relative to the average ultimate stress. The maximum standard deviation value of Young's modulus was 18.6 GPa at 400 °C, corresponding to a value of 17.4% with respect to the average Young's modulus. It can be seen that all standard deviation values are acceptable in the application of composite materials for construction.

3.1.3. Results of the GC3 textile specimens

Fig. 8 shows the thermomechanical behaviour of the GC3 carbon textile. The results were obtained from the direct tensile tests carried out at different temperature levels varying from 25 °C to 500 °C. In this figure, for each temperature level, there is an average "stress–thermomechanical strain" curve that was selected among the curves obtained from the direct tensile tests in the same thermomechanical condition on the GC3 textile specimens. In the results, the GC3 carbon textile always gave typical behaviour characterized by two properties: ultimate stress and Young's modulus. The test specimen failure was easily noticed by the stress drop on the "stress–thermomechanical strain" curve. This fragile failure mode normally could be found in the tests of carbon fibre products.

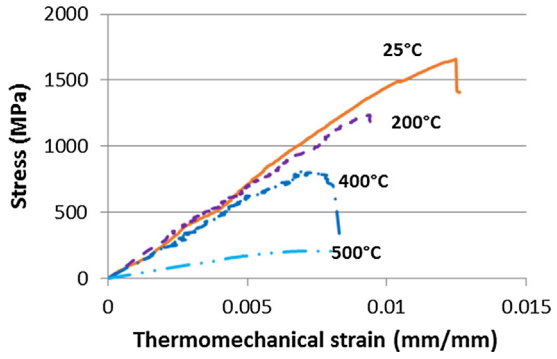

Fig. 8. Thermomechanical behaviour of the GC3 carbon textile: stress–thermomechanical strain relationship at different temperatures (25 °C, 200 °C, 400 °C, 500 °C).

Regarding the ultimate stress of the GC3 carbon textile, there is a decrease as a function of the temperature. The average stress obtained at 25 °C was 1442.7 MPa, whereas this value of the tests at 500 °C was 204.3 MPa, corresponding with 14.2% relative to itself at 25 °C (see Table 5). In the temperature levels ranging from 400 °C to 500 °C, a clear reduction of the ultimate stress can be seen in Fig. 8. Other values of the GC3 carbon textile stress are shown in Table 5.

In the experimental results, the slope of the "stress–thermomechanical strain" curve (or Young's modulus) of the GC3 carbon textile decreases when the temperature increases. Young's modulus varies from 130.2 GPa (average value at 25 °C) to 32 GPa (average value at 500 °C). This value does not decrease significantly for temperature levels ranging from 25 °C to 400 °C (approximately 30%), but it greatly decreases at temperatures over 400 °C, which causes a very low value at 500 °C. Table 5 presents the experimental results on the GC3 carbon textile. In this table, the average values and the standard deviation values of Young's modulus and ultimate stress data were calculated. The maximum standard deviation value of the GC3 carbon textile of the ultimate stress data was 242.2 MPa at 25 °C, corresponding to 16.8% of its average ultimate stress at 25 °C. The maximum standard deviation value for the Young's modulus data of the GC3 carbon textile was 25.4 GPa at 200 °C, corresponding to 21.6% of its average Young's modulus at 25 °C.

3.2. Evolution of the thermomechanical properties as a function of temperature

Figs. 6–8 show the **tensile tress** evolution of three carbon textiles as a function of temperature. The normalized mechanical properties (normalized ultimate stress and Young's modulus) are defined as the ratio between the mechanical property at a temperature (T) and that at room temperature (σ_T/σ_{25} or E_T/E_{25}). The normalized mechanical properties of three studied carbon textiles are tabulated in Table 4 and plotted in Figs. 9 and 10. Three carbon textiles gave reductions of the normalized ultimate stress values that are similar when the temperature increases from 25 °C to 400 °C. At 200 °C, the ultimate stress of the carbon textile (GC1, GC2 or GC3) remained 82.9%, 87.9% or 81.0%, respectively, of its ultimate

Table 5
Results of the direct tensile tests performed on the GC3 carbon textile.

Sample's ID	T °C	Tempe-rature increase rate (°C/min)	Ultimate stress (MPa)	Average stress (MPa)	Standard deviation (MPa)	Young's modulus (GPa)	Average modulus (GPa)	Standard deviation (GPa)
GC3 – 25 °C - a	25	0	1182.1	1442.7	242.2	135.6	130.2	7.1
GC3 – 25 °C - b			1485.3			122.1		
GC3 – 25 °C - c			1660.8			133.0		
GC3 – 200 °C - a	200	6.40	1234.1	1168.1	103.0	143.8	117.4	25.4
GC3 – 200 °C - b			1221.6			93.2		
GC3 – 200 °C - c			1049.7			115.1		
GC3 – 400 °C - a	400	13.31	948.5	845.9	89.1	85.8	95.9	21.6
GC3 – 400 °C – b			802.0			120.7		
GC3 – 400 °C – b			787.3			81.0		
GC3 – 500 °C – a	500	16.31	204.3	185.7	18.6	32.0	38.4	6.4
GC3 – 500 °C – b			167.1			44.8		
GC3 – 500 °C – c			NA			NA		
GC3 – 600 °C – a	600	–	NA	–	–	NA	–	–
GC3 – 600 °C – b			NA			NA		

NA: not available.

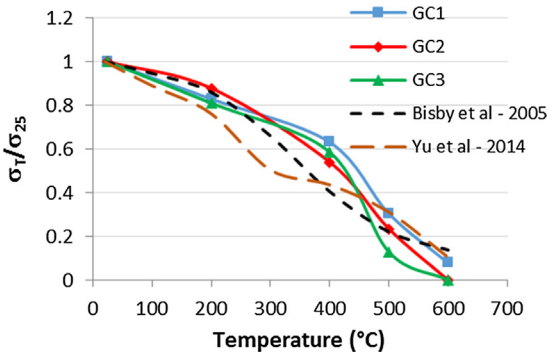

Fig. 9. Evolution of normalized ultimate stress obtained for the studied carbon textiles compared with experimental results on the CFRP composite materials obtained by Bisby et al. 2005 [36], by Yu et al. 2014 [38].

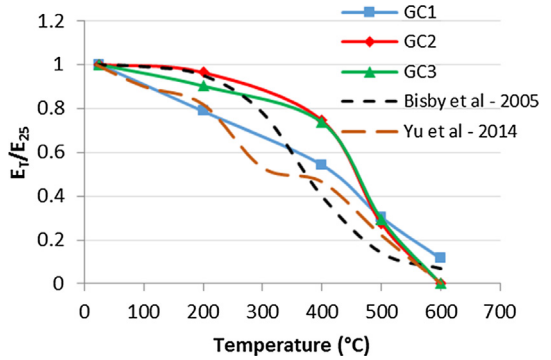

Fig. 10. Evolution of normalized Young's modulus obtained for the studied carbon textiles compared with experimental results on the CFRP composite materials obtained by Bisby et al. 2005 [36], by Yu et al. 2014 [38].

stress at room temperature. At 400 °C, the normalized ultimate stresses were 63.1%, 54.0%, and 58.6% for GC1, GC2, and GC3, respectively. At temperatures above 400 °C, the GC1 textile gave better behaviour than the other two textiles (GC2 and GC3). At 500 °C, this carbon textile retained 32.5% of its ultimate stress value at 25 °C, whereas the other two textiles provided an ultimate stress less than 22% compared with the ambient temperature value. At 600 °C, the GC1 carbon textile was not broken under thermal action; its tensile stress reached 7.8% relative to the ambient temperature value. The GC2 and GC3 carbon textiles were always broken in the second phase (thermal exposure) of the test procedure at 600 °C, and the experimental data could not be obtained. Fig. 9 shows the evolution of the normalized ultimate stress of three carbon textiles as a function of temperature compared with the other experimental results on the CFRP composite materials obtained by Bisby et al. 2005 [36] and by Yu et al. 2014 [38]. In Fig. 9, the ultimate stress evolution of the GC1 and GC3 carbon textiles can be divided into two zones. At temperatures ranging from 25 °C to 400 °C, the ultimate stress slightly decreased as a function of temperature. At 200 °C, these two textiles retained approximately 80% of its ultimate stress at room temperature, whereas this normalized ultimate stress was approximately 60% at 400 °C. At temperatures ranging from 400 °C to 600 °C, there was a substantial reduction in the ultimate stress. The complete decomposition of pre-impregnated products in carbon textiles caused this considerable reduction. Fig. 10 shows the normalized Young's modulus of three carbon textiles as a function of temperature. It can be found that there was almost the same evolution of Young's modulus as a function of temperature between the GC2 and GC3 carbon textiles. The normalized Young's modulus values were 96.4% (GC2) and 90.1% (GC3) at 200 °C, 74.4% (GC2) and 73.6% (GC3) at 400 °C, and 23.8% (GC2) at 500 °C. The GC1 carbon textile gave a nearly linear decrease in Young's modulus as a function of temperature. The normalized Young's moduli of the GC1 carbon textile were 78.7%, 54.2%, 30.3%, and 11.5% at 200 °C, 400 °C, 500 °C, and 600 °C, respectively. All values of the normalized mechanical properties of three carbon textiles are presented in Table 6 below.

Table 6
Evolution of the normalized mechanical properties of three carbon textiles as a function of temperature.

T °C	Normalized ultimate stress σ_T/σ_{25} (%)			Normalized Young's modulus E_T/E_{25} (%)		
	GC1	GC2	GC3	GC1	GC2	GC3
25	100	100	100	100	100	100
200	82.9	87.9	81.0	78.7	96.4	90.1
400	63.1	54.0	58.6	54.2	74.4	73.6
500	30.4	21.1	12.9	30.3	23.8	29.5
600	7.8	0	0	11.5	0	0

For the evolution of Young's modulus with temperature in Fig. 10, the influence of temperature on Young's modulus of the GC2 and GC3 carbon textiles could be divided into two temperature intervals. The first interval, from 25 °C to 400 °C, was described by a slight reduction of Young's modulus. At 400 °C, the stiffness of carbon textiles GC2 and GC3 converted approximately 75% compared with that obtained at ambient temperature. In the second interval, from 400 °C to 600 °C, Young's modulus greatly decreased and was almost negligible at 600 °C. Concerning the Young's modulus evolution of the GC1 carbon textile as a function of temperature, this textile had a progressive reduction when the temperature increased. Fig. 10 shows only one almost linear reduction of Young's modulus as a function of temperature.

3.3. Failure modes

The samples of three studied carbon textiles after the tests at different temperatures are observed to present the failure modes of the three textiles. The results revealed two main failure modes for the three carbon textiles. This argument is consistent with the results available in the literature [50]. The failure modes of the three carbon textiles are illustrated in Fig. 11.

At a temperature level below 400 °C, the three carbon textiles exhibited a brittle failure mode marked by a drop in stress on the "stress–thermomechanical strain" curve (see Fig. 6 (GC1), Fig. 7 (GC2), Fig. 8 (GC3)). The treatment products in the three textiles do not yet begin to decompose, so they ensure good load transmission in carbon monofilaments. This main reason helps carbon textiles retain their mechanical properties (especially Young's modulus) in the temperature range from 25 °C to 400 °C (see Fig. 10). At a temperature level above 400 °C, owing to the damage of the polymer resin and oxidation of carbon fibre, the carbon textiles become more softened and separated, which causes a significant reduction in ultimate stress and Young's modulus. In Fig. 11, the carbon textiles are partially oxidized at 500 °C and 600 °C, and the test specimens of the three textiles are grounded by the fibre stretching. For the GC2 and GC3 carbon textiles, after reaching the maximum value, the stress progressively decreases as a function of the deformation on the "stress–thermomechanical strain" curve. The progressive failure of each monofilament in the textile is caused mainly by this failure mode. The GC1 carbon textile samples sometimes exhibit a brittle fracture mode at 500 °C (see Fig. 6) because the polymer resin pre-impregnated in this textile is not yet completely decomposed, which ensures a co-working of the textile filaments.

a) GC1 carbon textile

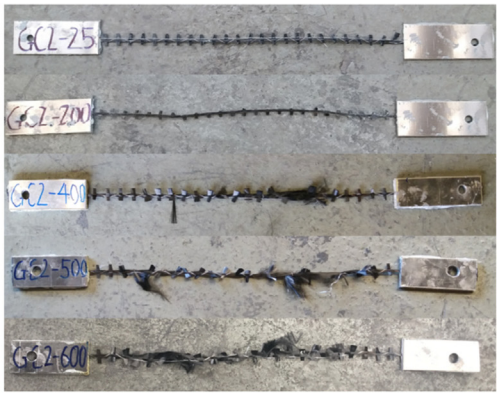

b) GC2 carbon textile

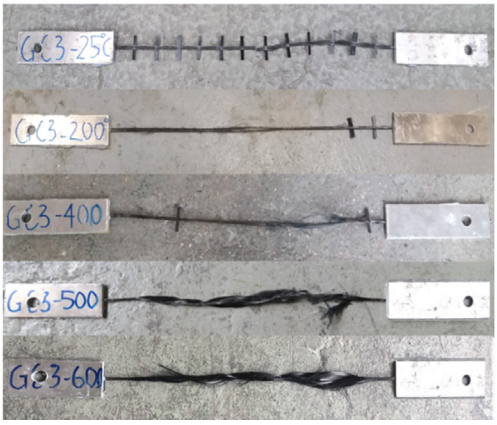

c) GC3 carbon textile

Fig. 11. Failure modes of the test specimens of three carbon textiles at various temperatures.

3.4. Discussion

This section presents discussions to explain the effect of carbon fibre treatment products on the results obtained (ultimate strength and Young's modulus, thermomechanical property evolution depending on temperature, and failure modes of three carbon textile specimens), which were presented in Section 3.3.

3.4.1. Ultimate stress and Young's modulus of the carbon textiles

According to the results obtained on the ultimate stress and Young's modulus of the three carbon textiles presented in Section 3.1, the influence of treatment by different products on the behaviour of these carbon textiles at elevated temperatures can be determined. Three studied carbon textiles have almost equivalent cross-sections for a textile yarn. The GC1 carbon textile has an important load capacity and good rigidity owing to its very good pre-impregnation with an epoxy resin product. This very good pre-impregnation has assured a good load transmission between the monofilaments of the GC1 carbon textile yarn. The ultimate stress of the GC1 textile was always 1.8 times the value of the other two textiles. The ratio of ultimate stress between the GC1 and GC2 textiles has varied from 1.9 (at 200 °C) to 2.6 (at 500 °C) as a function of the temperature, whereas this ratio between the GC1 and GC3 textiles was in the range of 1.8 (at 25 °C) to 4.3 (at 500 °C). Regarding the pre-impregnation of the GC2 and GC3 textiles, they are coated with an amorphous silica (for GC2) and epoxy resin with very low content (for GC3). This reduced the bonding between the monofilaments in a textile yarn, which caused less load-carrying capacity than the GC1 carbon textile. At a temperature higher than 400 °C, the epoxy resin pre-impregnated in the GC1 carbon textile began to burn partially, but its load-transmitting capacity is much better than the other two carbon textiles. This gave a great ratio value of the ultimate stress between the GC1 carbon textile and the others at elevated temperatures. Concerning the stiffness of carbon textiles, the influence of the pre-impregnated product on Young's modulus could also be found. In the experimental results, as a function of the temperature level, Young's modulus of the GC1 carbon textile was 1.3 to 1.9 times greater than the GC2 textile and 1.5 to 2.0 times greater than the GC3 textile. There is a good relationship between the miles mono-filaments of the GC1 textile yarn, which could provide a joint working ability in the longitudinal direction of the GC1 carbon textile. This capacity has caused a higher stiffness value of GC1 than the other textiles (GC2, GC3) as presented above. The coating treatment in the GC2 and GC3 textiles gave a similar effect on the thermomechanical behaviour of carbon textile. The ultimate stress and Young's modulus of two carbon textiles (GC2, GC3) are approximately similar.

3.4.2. Evolution of the ultimate stress and Young's modulus of the carbon textiles depending on the temperature

The experimental results showed that the thermomechanical properties of carbon textiles decrease as a function of temperature. Consequently, the effect of temperature on these decreases was different for each studied carbon textile. The evolution of the ultimate stress and/or Young's modulus depended on the coating

treatment and the pre-impregnation rate of the carbon textiles. Regarding the reduction of the ultimate stress, the carbon textiles treated with the resin product gave a typical evolution depending on the temperature. This evolution can be divided into two stages: a slight reduction (approximately 40%) in the temperature range from 25 °C to 400 °C and a very important decrease at temperatures of 400 °C to 600 °C. If the textile has been perfectly impregnated in the epoxy resin (GC1 textile), the carbon textile ultimate stress could remain approximately 30.4% at 500 °C and 7.8% at 600 °C compared with that at ambient temperature. The normalized ultimate stress of the GC3 carbon textile was 12.9% at 500 °C and almost zero at 600 °C. This means that the impregnated ratio significantly influenced the evolution of the ultimate stress at elevated temperatures (see Fig. 9). On the other hand, in the first stage (from 25 °C to 400 °C), the normalized ultimate stress of two carbon textiles (GC1 and GC3) was approximately similar. These values were respectively 82.9% and 81.0% at 200 °C and 63.1% and 58.6% at 400 °C for these two carbon textiles (GC1 and GC3). The similarity between the ultimate stress evolution of two carbon textiles (GC1 and GC3) in this case could be explained by a significant contribution of the impregnated resin, which can ensure good charge transmission between monofilaments. Concerning the ultimate stress evolution of the GC2 carbon textile, which was impregnated by an amorphous silica product as a coating, the ultimate stress has decreased in a somewhat curved way (see Fig. 9). The influence of the elevated temperature on this treatment product was not significant for an important reduction at elevated temperatures. The application of this product as coating has the object of improving the bond between the carbon textile and the matrix of the concrete in the manufacture of the composite TRC. Fig. 10 shows that the decrease in Young's modulus of the GC2 and GC3 textiles was similar. This evolution began with a step of a slight reduction (approximately 25%) in the temperature range from 25 °C to 400 °C and finally a step from a very significant decrease to a negligible value at 600 °C. These results could be explained by the contribution of the treatment products of two carbon textiles to their stiffness. At moderate temperatures from 25 °C to 400 °C, the contribution of the impregnated epoxy resin to GC3 carbon textile stiffness was still good, so there was some difference between the normalized Young's modulus values of two textiles (76.4% for GC2 and 73.6% for GC3). At temperatures above 400 °C, the decomposition of impregnated resin in the temperature range from 400 °C to 450 °C caused a slight contribution in the GC3 carbon textile stiffness as the role of amorphous silica product in GC2 carbon textile. The GC2 and GC3 carbon textiles therefore had the same evolution of Young's modulus as a function of temperature. In the results, the impregnated resin contribution in a GC1 textile yarn caused a nearly linear Young's modulus reduction as shown in Fig. 10. The effect of temperature on the resin matrix significantly influenced Young's modulus of the GC1 carbon textile. At a moderate temperature (from 25 °C to 400 °C), the impregnated resin was gradually softened, which caused a lesser contribution to carbon textile stiffness. At an elevated temperature above 400 °C, the GC1 carbon textile was gradually decomposed and burned until its complete decomposition, which largely influenced the working in common between carbon monofilaments.

3.4.3. Failure modes

All three carbon textile samples in the test campaign were presented in Section 3.3. Two failure modes could be found on the specimen images after the tests. With respect to the failure mode of the GC1 carbon textile, at moderate temperatures (from 25 °C to 400 °C), the pre-impregnated resin within a yarn was not completely decomposed and thus can work in common between carbon monofilaments. The specimen was broken in an abrupt way which is called fragile rupture mode when the material reached a limited state. This failure mode was clearly characterized by a significant drop in the stress on the "stress–thermomechanical strain" curve of the GC1 textile (see Fig. 6). This means that most of the monofilaments were broken at the same time in a GC1 textile yarn, and the test specimens after the test were either completely broken by the rupture energy, such as those at 25 °C, or partially destroyed and capable of withstanding the mechanical loads after cooling, such as those at 200 °C and 500 °C. At an elevated temperature level above 500 °C, the GC1 carbon textile had a different failure mode as illustrated in Fig. 11-a. The pre-impregnated epoxy resin was completely decomposed, the carbon monofilaments remained single, and there is no connection between them. This could explain the failure mode in which the rupture energy was progressively liberated by the breakage of each monofilament in a textile yarn after the complete decomposition of the pre-impregnated resin. The deformation of the sample increased, whereas the stress decreased progressively. It could be said that the failure mode in this case is ductile. The GC3 carbon textile featured two failure modes similar to the GC1 textile, but with a low level of pre-impregnated resin, it featured a ductile failure mode at a temperature level higher than 400 °C, and the samples were broken on all mono-filaments. In the temperature range from 25 °C to 400 °C, there was still some pre-impregnated resin in the specimens after the tests. The failure mode could be explained similarly to the GC1 carbon textile (see Fig. 11-c). As shown in Fig. 11-b, the GC2 carbon textile provided a single failure mode because the coating with amorphous silica was not greatly influenced by the action of the elevated temperature. The samples thus badly retained their initial form. A low contribution of amorphous silica in the textile load capacity was another reason for these results. The damage appeared in a GC2 textile yarn from each group of monofilaments that had less charge capacity than the others. This means that the rupture energy was progressively liberated in part on each group of monofilaments. The cooled test specimens could support the mechanical load, but the residual resistance obtained would decrease when the temperature of test increased.

4. Analytical modelling

The experimental results obtained from the tests of three carbon textiles are used to develop an analytical model of the temperature influence on the ultimate stress and Young's modulus of three textiles. In the literature, some authors have proposed analytical models to predict the evolution of mechanical properties (ultimate stress, Young's modulus) as a function of temperature. Normally, this mechanical property reduction relation is in the form of either a hyperbolic tangent function or an exponential function. All studies on analytical models of the evolution of mechanical properties dependent on temperature are summarized in the work of Gibson [50] and Firmo et al. [51]. Bisby [52] proposed a semi-empirical sigmoid function to predict the temperature-dependent reduction of the resistance and/or Young's modulus of the FRP composite. In his model, the parameters are the empirically derived coefficients. Wang et al. [37] recently developed a model (originally for metals) to determine the tensile strength of CFRP at high temperatures. Another author is Mahieux et al. [53], who gave a relationship in the form of a temperature-dependent function to calculate the high temperature resistance.

In this paper, the authors calibrated the Mouritz and Gibson model [54] with the experimental data on three carbon textiles. The reduction relationship of mechanical properties as a function of temperature is described by the following equation:

$$P(T) = R^n\left[\frac{P_u + P_r}{2} - \frac{P_u - P_r}{2}\tanh\left(K_m(T - T_g)\right)\right] \quad (1)$$

where P(T) is a mechanical property at temperature T (ultimate tensile strength and Young's modulus); Pu is a value of this property at the lowest temperature of the experiment (normally at ambient temperature); Pr is the value of this property at the temperature after thermal damage of the material (or after the glass transition for fibre-reinforced polymer) but before decomposition; Km is a coefficient to be determined as a function of the experimental results; Tg is the temperature around which the curve is quasi-symmetric, normally corresponding to a 50% reduction in the property value, to be modified as a function of the experimental results; R is a coefficient that depends on the matrix and varies between 0 and 1; and n is a parameter that depends on the stress state (n = 1 when the properties of the resin dominate, n = 0 when the properties of the fibres dominate) [51,54].

Regarding the GC1 carbon textile samples before the tests, it can be seen that the epoxy resin pre-impregnated in this textile was burned completely at 600 °C, and the ultimate stress and Young's modulus of the GC1 carbon textile at 600 °C were used as the Pr value. The critical temperatures (Tg) corresponding to a 50% reduction in ultimate strength and Young's modulus are 443 °C and 418 °C, respectively. The Km parameter in the analytical model of the GC1 carbon textile is determined by the experimental results obtained. This parameter value varies as a function of the temperature and is 0.004 and 0.01 for the temperature ranges of 25 °C to 500 °C and 500 °C to 600 °C, respectively, in the ultimate strength model and 0.0035 and 0.008 for the temperature ranges from 25 °C to 500 °C and from 500 °C to 600 °C, respectively, in the Young's modulus model (see Table 7). Regarding the parameters for the analytical model of the GC2 carbon textile, the ultimate strength and Young's modulus of GC2 carbon textile at 500 °C are chosen as the Pr value because the amorphous silica-coated product of this textile was completely decomposed at 500 °C. The temperature Tg for the analytical model in this case is 405 °C for the ultimate strength and 448 °C for Young's modulus. The parameter Km is a temperature-dependent coefficient, and the experimental data on the GC2 carbon textile is presented in Table 6. Table 7 presents all parameters of the analytical model for the third carbon textile (GC3). The Pu values in two analytical models (ultimate strength and Young's modulus) in this case are 1442.72 MPa and 130.22 GPa, corresponding to its ultimate strength and Young's modulus at 25 °C. The GC3 carbon textile results at 500 °C are used as the Pr values for both analytical models.

Fig. 12 compares the tensile strength predicted from the proposed empirical relationships with the measured values of the experiment. In the results, the proposed empirical relationships closely match the data measured for the three carbon textiles. The average errors between the predicted maximum strength and the test data are 11.1%, 6.5%, and 4.7% for three textiles GC1, GC2, and GC3, respectively. The maximum error between the test data and empirical equations occurred for the GC1 carbon textile at 600 °C with a value of 21.8%. The standard deviations for three carbon textiles are 9.8%, 5.1%, and 1.9%, respectively (see Table 7). All these values demonstrate a reasonable agreement between test data and empirical equations. Concerning the analytical model of Young's modulus for the three textiles, Fig. 13 shows the Young's modulus evolution as a function of temperature by comparison with the predicted modulus values from the Gibson model. It can be found that the curves of the analytical model are always in the zones created by the experimental curves of the three textiles and their standard deviations.

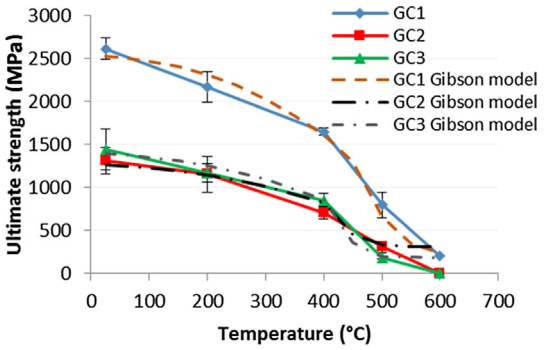

Fig. 12. Comparison of tensile strength predicted by the Gibson model with test data on three studied carbon textiles (GC1, GC2, GC3) as a function of temperature.

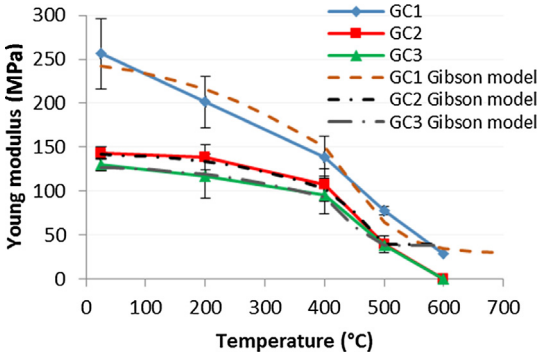

Fig. 13. Comparison of Young's modulus predicted by the Gibson model with test data on three carbon textiles as a function of temperature.

Table 7
Parameters of the analytical model for three carbon textiles.

Material	Mechanical property	Parameters			
		Pu (MPa)	Pr (MPa)	Tg (°C)	Km
GC1	Ultimate stress	2616.6	204.9	443	0.004 ($25 \le T \le Tg$) 0.013 ($Tg < T \le 600$)
	Young's modulus	256.2	29.5	418	0.0035 ($25 \le T \le Tg$) 0.0103 ($Tg < T \le 600$)
GC2	Ultimate stress	1311.5	277.4	405	0.004 ($25 \le T \le Tg$) 0.02 ($Tg < T \le 600$)
	Young's modulus	143.8	34.2	448	0.0045 ($25 \le T \le Tg$) 0.15 ($Tg < T \le 600$)
GC3	Ultimate stress	1442.7	204.3	419	0.004 ($25 \le T \le Tg$) 0.03 ($Tg < T \le 600$)
	Young's modulus	130.2	32.0	448	0.004 ($25 \le T \le Tg$) 0.3 ($Tg < T \le 600$)

Table 8
Comparison between the two results: experimentation and analytical model.

Mate-rial	Temperature	Ultimate stress			Young's modulus		
		Experiment (MPa)	Analytical (MPa)	Errors (%)	Experiment (%)	Analytical (%)	Errors (%)
GC1	25	2616.6	2534.4	3.1	256.2	242.6	5.3
	200	2169.5	2314.6	6.7	201.6	215.7	7.0
	400	1652.2	1616.1	2.2	138.8	150.0	8.1
	500	795.7	651.4	18.1	77.6	65.1	16.2
	600	204.9	245.0	19.5	29.5	34.8	18.0
	Average error			**9.9**			**10.9**
	Standard deviation			**8.3**			**5.75**
GC2	25	1311.5	1265.7	3.5	143.8	141.6	1.6
	200	1152.5	1148.5	0.4	138.6	133.7	3.5
	400	708.8	819.9	15.7	107.1	102.9	3.9
	500	308.1	330.1	7.1	39.7	39.7	0.00
	Average error			**6.7**			**2.3**
	Standard deviation			**5.8**			**2.2**
GC3	25	1442.7	1391.2	3.6	130.2	127.2	2.3
	200	1168.5	1256.9	7.6	117.4	119,1	1,5
	400	845.9	961.9	1.9	95.9	93,0	3,0
	500	185.8	195.4	5.2	38.4	38.4	0.0
	Average error			**4.6**			**1.7**
	Standard derivation			**2.2**			**1.1**

In Table 8, the predicted Young's modulus by the proposed empirical relationship is compared with the experimental data. The average error and standard deviation of Young's modulus between the proposed empirical relationships and the measured values of the experiment are also calculated. The maximum error value (by percentage) between the two results is 18.8% for the GC1 carbon textile at 500 °C. The average errors between the predicted Young's modulus and the test data are 11.4%, 2.9%, and 2.2% for the three textiles GC1, GC2, and GC3 respectively. The standard deviation values in these cases are 6.4%, 2.8%, and 2.2%, respectively, for the three textiles GC1, GC2, and GC3. All the values concerning the comparison between the two results of the experiment and the analytical model are presented in the Table 8.

5. Conclusions and future works

The objective of this work is to identify the thermomechanical behaviour of carbon textiles subjected to mechanical and thermal loads. Carbon textiles are usually used in the manufacture of textile-reinforced concrete composite (TRC). Three carbon textiles (GC1, GC2, GC3) were tested under thermomechanical loading at five temperature levels (25 °C, 200 °C, 400 °C, 500 °C, and 600 °C). All thermomechanical properties such as ultimate stress, Young's modulus, and thermomechanical strain were identified and presented. The notable difference among three carbon textiles was the treatment by products of different natures. The GC1 and GC3 textiles were pre-impregnated by epoxy resin with two different pre-impregnation ratios, completely pre-impregnated for the GC1 textile and a very low level for GC3 textile, whereas the GC2 textile was treated with a product of amorphous silica as a coating.

Other problems presented in this paper are the influence of the treated product on the thermomechanical behaviour, the evolution of the thermomechanical properties as a function of the temperature, and the failure mode of the carbon textile samples. With complete pre-impregnation by the epoxy resin, the GC1 carbon textile possessed ultimate stress and Young's modulus approximately 2 and 1.8 times greater than the other textiles, respectively. Regarding the evolution of the textile mechanical properties as a function of temperature, an almost linear reduction can be found for Young's modulus of the GC1 textile, whereas the GC2 and GC3 textiles featured an evolution with two steps: the first step with a slight reduction (approximately 20%) in the temperature range from 25 °C to 400 °C, and the second step with a very large decrease to a negligible value at 600 °C. For the ultimate stress, the GC1 and GC3 carbon textiles, which were treated with an epoxy resin product, exhibited almost the same evolution as a function of temperature. With the treatment of amorphous silica as a coating, which was not significantly influenced by thermal action, the GC2 textile had a curved evolution as a carbon fibre. The fracture modes were also analysed in this paper by observing all samples after the tests at different temperatures. Thus, the influence of the treatment product on failure modes of the carbon textiles could be determined. A fragile failure mode was observed in the temperature range from 25 °C to 400 °C in the carbon textiles treated with the epoxy resin product (GC1 and GC3). This failure mode is clearly characterized by a drop in stress in the "stress–thermomechanical strain" relationship even if the test piece has not yet completely broken. At higher temperatures, these two carbon textiles (GC1 and GC3) exhibited a ductile failure mode of the specimens, which was characterized by the progressive damage of each monofilament within a carbon yarn. The same mode of rupture was observed on samples of the GC2 carbon textile at elevated temperatures. Regarding the treatment product as a reason for this result, the amorphous silica was not strongly influenced by the temperature.

To clearly characterize the evolution of thermomechanical properties as a function of temperature, the analytical model of Mouritz and Gibson was calibrated with experimental results obtained on three studied carbon textiles. The parameters in this model, such as Pr, Pu, Tg, and Km, were determined from the ultimate stress and Young's modulus of the experimental data. For the Tg parameter value, it was always in the temperature range from 400 °C to 450 °C. The results predicted by this analytical model were reasonable compared with those obtained experimentally. The average error and standard deviation values were calculated and analysed; an agreement between the analytical modelling results and the experimental results was obtained in this study.

For future works, it will be interesting to manufacture textile-reinforced concretes (TRCs) based on the refractory concrete matrix and reinforced by the GC1 and GC2 carbon textiles to study the influence of the textile type on its thermomechanical behaviour at elevated temperatures.

Acknowledgments

This research has been performed with the financial support of LMC2 (thanks to its industrial projects) for the experimental works. This research has also been realized with the financial support of a doctoral scholarship from the Ministry of Education and Training of Vietnam to the first author. We would like to thank the team of technicians (Mr. E. JANIN and Mr. N. COTTET) from the Civil Engineering department of IUT Lyon 1 and LMC2, University of Lyon 1 for their technical support.

References

[1] L. Bisby, M. Green, V. Kodur, Response to fire of concrete structures that incorporate FRP, Prog. Struct. Eng. Mater. 7 (2005) 136–149.
[2] V. Mechtcherine, Novel cement-based composites for the strengthening and repair of concrete structures, Constr. Build. Mater 41 (2013) 365–373 (Review article).
[3] M. Butler, M. Lieboldt, V. Mechtcherine, Application of textile-reinforced concrete (TRC) for structural strengthening and in prefabrication, in: G. van Zijl, W.P. Boshoff (Eds.), Advances in Cement-Based Materials, Taylor & Francis Group, London, 2010, pp. 127–136.
[4] W. Brameshuber. Textile Reinforced Concrete. RILEM Report 36. State-of-the-Art" Report of RILEM Technical Committee, TC 201-TRC.T, 2006.
[5] K. Acatay, Carbon fibers. Fiber technology for fiber-reinforced composites, Compos. Sci. Eng. (2017) 123–151.
[6] B.A. Newcomb, Processing, structure, and properties of carbon fibers, Compos. A Appl. Sci. Manuf. 91 (2016) 262–282.
[7] O. Awani, T. El-Maaddawy, N. Ismail, Fabric-reinforced cementitious matrix: a promising strengthening technique for concrete structures, Constr. Build. Mater. 132 (2017) 94–111.
[8] I.G. Colombo, M. Colombo, M. Di Prisco, Bending behaviour of Textile Reinforced Concrete sandwich beams, Const. Build. Mater. 95 (2015) 675–685.
[9] J. Blom, M. El Kadi, J. Wastiels, D.G. Aggelis, Bending fracture of textile reinforced cement laminates monitored by acoustic emission: influence of aspect ratio, Const. Build. Mater. 70 (2014) 370–378.
[10] A. Peled, Z. Cohen, Y. Pasder, A. Roye, T. Gries, Influences of textile characteristics on the tensile properties of warp knitted cement based composites, Cem. Concr. Compos. 30 (2008) 174–183.
[11] T. Hulin, D.H. Lauridsen, K. Hodicky, J.W. Schmidt, H. Stang, Influence of basalt FRP mesh reinforcement on high-performance concrete thin plates at high temperatures, J. Compos. Constr. 20 (1) (2015).
[12] D. Ehlig, F. Jesse, M. Curbach. High temperature tests on textile reinforced concrete (TRC) strain specimens. In: W. Brameshuber (Eds.), 2nd ICTRC, Textile Reinforced Concrete. Proceeding of the Inter. RILEM Conf. on Material Science (MatSci) v.I (PRO 75), RILEM. Publications SARL, Aachen, 2010:141-51.
[13] T Büttner, Orlowsky J, Raupach M. Fire resistance tests of textile reinforced concrete under static loading – results and future developments, in: Proceeding of the 5th Inter. RILEM Workshop on High Performance Fiber Reinforced Cement Composites (HPFRCC5); 2014:361-70.
[14] H.W. Reinhardt, M. Krüger, M. Raupach, Behavior of textile-reinforced concrete in fire, ACI Special Publ. 250 (2008) 99–110.
[15] D.A.S. Rambo, Y. Yao, F.d.A. Silva, R.D.T. Filho, B. Mobasher, Experimental investigation and modelling of the temperature effects on the tensile behavior of textile reinforced refractory concretes, Cem. Concr. Compos. 75 (2017) 51–61.
[16] S. Xu, L. Shen, J. Wang, The high-temperature resistance performance of TRC thin-plates with different cementitious materials: experimental study, Constr. Build. Mater. 115 (2016) 506–519.
[17] I. Colombo, M. Colombo, A. Magri, G Zani, M.di Prisco. Textile reinforced mortar at high temperatures, in: Applied Mechanics and Materials. Trans Tech Publications, 2011:202-07.
[18] J. Blom, J.V.Ackeren, Wastiels J. Study of the bending behavior of textile reinforced cementitious composites when exposed to high temperatures, in: Proceeding of the 2nd Inter. RILEM Conference on Strain Hardening Cementitious Composites (SHCC2-Rio), 2011.
[19] J. Donnini, F.D.C. Basalo, V. Corinaldesi, G. Lancioni, A. Nanni, Fabric-reinforced cementitious matrix behavior at high-temperature: experimental and numerical results, Compos. B Eng. 108 (2017) 108–121.
[20] D.A.S. Rambo, F.A. Silva, R.D.T. Filho, N. Ukrainczyk, E. Koenders, Tensile strength of a calcium-aluminate cementitious composite reinforced with basalt textile in a high-temperature environment, Cem. Concr. Compos. 70 (2016) 183–193.
[21] T.H. Nguyen, X.H. Vu, A.S. Larbi, E. Ferrier, Experimental study of the effect of simultaneous mechanical and high-temperature loadings on the behaviour of textile-reinforced concrete (TRC), Constr. Build. Mater. 125 (2016) 253–270.
[22] Zoi C. Tetta, Dionysios A. Bournas, TRM vs FRP jacketing in shear strengthening of concrete members subjected to high temperatures, Compos. B Eng. 106 (2016) 190–205.
[23] Saad M. Raoof, Dionysios A. Bournas, TRM versus FRP in flexural strengthening of RC beams: Behaviour at high temperatures, Constr. Build. Mater. 154 (2017) 424–437.
[24] Saad M. Raoof, Dionysios A. Bournas, Bond between TRM versus FRP composites concrete at high temperatures, Compos. Part B: Eng. 127 (2017) 150–165.
[25] P. Tranchard, F. Samyn, S. Duquesne, M. Thomas, B. Estèbe, J.L. Montès, S. Bourbigot, Fire behaviour of carbon fibre epoxy composite for aircraft: Novel test bench and experimental study, J. Fire Sci. 33 (2015) 247–266.
[26] S. Timme, V. Trappe, M. Korzen, B. Schartel, Fire stability of carbon fiber reinforced polymer shells on the intermediate-scale, Compos. Struct. 178 (2017) 320–329.
[27] S.E. Boyd, S.W. Case, J.J. Lesko, Compression creep rupture behaviour of a glass/vinylester composite subject to isothermal and one-sided heat flux conditions, Compos. A Appl. Sci. Manuf. 38 (2007) 1462–1472.
[28] J.V. Bausano, S.E. Boyd, J.J. Lesko, S.W. Case, Composite life under sustained compression and one sided simulated fire exposure: characterization and prediction, Sci. Eng. Compos. Mat. 12 (2011) 131–144.
[29] S. Feih, A. Mouritz, Tensile properties of carbon fibres and carbon fibre–polymer composites in fire, Compos. A Appl. Sci. Manuf. 43 (2012) 765–772.
[30] A. Mouritz, S. Feih, E. Kandare, Z. Mathys, A. Gibson, P.D. Jardin, S. Case, B. Lattimer, Review of fire structural modelling of polymer composites, Compos. A Appl. Sci. Manuf. 40 (2009) 1800–1814.
[31] T. Bhat, V. Chevali, X. Liu, S. Feih, A. Mouritz, Fire structural resistance of basalt fibre composite, Compos. A Appl. Sci. Manuf. 71 (2015) 107–115.
[32] K. Grigoriou, A.P. Mouritz, Influence of ply stacking pattern on the structural properties of quasi-isotropic carbon-epoxy laminates in fire, Compos. A Appl. Sci. Manuf. 99 (2017) 113–120.
[33] S. Foster, L. Bisby, High temperature residual properties of externally bonded FRP systems, Special Publ. ACI 230 (2005) 1235–1252.
[34] M.F. Green, N. Bénichou, V.K.R. Kodur, L.A. Bisby. Design guidelines for fire resistance of FRP strengthened concrete structures, in: Eighth International Conference on FRP in Reinforced Concrete Structures (FRPRCS-8), Patras, Greece, 2007.
[35] S. Cao, Z. Wu, X. Wang, Tensile properties of CFRP and hybrid FRP composites at elevated temperatures, J. Compos. Mater. 43 (4) (2009) 315–330.
[36] L.A. Bisby, B.K. Williams, V.K.R. Kodur, M.F. Green, E. Chowdhury. Fire Performance of FRP Systems for Infrastructure: A state-of-the art report. NRC-CNRC, Research Report 179, Canada, 2005.
[37] K. Wang, B. Young, S.T. Smith, Mechanical properties of pultruded carbon fibre reinforced polymer (CFRP) plates at elevated temperatures, Engineer. Struct. 33 (2011) 2154–2161.
[38] B. Yu, V. Kodur, Effect of temperature on strength and stiffness properties of near-surface mounted FRP reinforcement, Compos. B Eng. 58 (2014) 510–517.
[39] P.L. Nguyen, X.H. Vu, E. Ferrier, Characterization of pultruded carbon fibre reinforced polymer (P-CFRP) under two elevated temperature-mechanical load cases: residual and thermo-mechanical regimes, Constr. Build. Mater. 165 (2018) 395–412.
[40] J.R. Correia, F.A. Branco, J.G. Ferreira, Y. Bai, T. Keller, Fire protection systems for building floors made of pultruded GFRP profiles: Part 1: Experimental investigations, Compos. B Eng. 41 (2010) 617–629.
[41] B.K. Kandola, P. Myler, A.R. Horrocks, M. El-Hadidi, D. Blair, Empirical and numerical approach for optimisation of fire and mechanical performance in fire-retardant glass-reinforced epoxy composites, Fire Saf. J. 43 (2008) 11–23.
[42] B.K. Kandola, A.R. Horrocks, P. Myler, D. Blair, Mechanical performance of heat/fire damaged novel flame retardant glass-reinforced epoxy composites, Compos. A Appl. Sci. Manuf. 34 (2003) 863–873.
[43] P. Behera, V. Baheti, J. Militky, S. Naeem, Microstructure and mechanical properties of carbon microfiber reinforced geopolymers at elevated temperatures, Const. Build. Mater. 160 (2018) 733–743.
[44] R.J.A. Hamad, M.A.M. Johari, R.H. Haddad, Mechanical properties and bond characteristics of different fiber reinforced polymer rebars at elevated temperatures, Constr. Build. Mater. 142 (2017) 521–535.
[45] M.D. Ludovico, F. Piscitelli, A. Prota, M. Lavorgna, G. Mensitieri, G. Manfredi, Improved mechanical properties of CFRP laminates at elevated temperatures and freeze–thaw cycling, Const. Build. Mater. 31 (2012) 273–283.
[46] H. Hajiloo, M.F. Green, J. Gales, Mechanical properties of GFRP reinforcing bars at high temperatures, Constr. Build. Mater. 162 (2018) 142–154.
[47] A. Agarwal, S.J. Foster, E. Hamed, Testing of new adhesive and CFRP laminate for steel-CFRP joints under sustained loading and temperature cycles, Compos. B Eng. 99 (2016) 235–247.
[48] B. Ghadimi, S. Russo, M. Rosano, Predicted mechanical performance of pultruded FRP material under severe temperature duress, Composite Structure 176 (2017) 673–683.
[49] S. Russo, B. Ghadimi, K. Lawania, M. Rosano, Residual strength testing in pultruded FRP material under a variety of temperature cycles and values, Compos. Struct. 133 (2015) 458–475.
[50] A.G. Gibson, Laminate theory analysis of composites under load in fire, J. Compos. Mater. 40 (7) (Jul. 2005) 639–658.
[51] J.P. Firmo, J.R. Correia, L.A. Bisby, Fire behaviour of FRP-strengthened reinforced concrete structural elements: A state-of-the-art review, Compos. B Eng. 80 (2015) 198–216.
[52] L.A. Bisby, Fire Behaviour of Fibre-Reinforced Polymer (FRP) Reinforced or Confined Concrete (PhD thesis), Queen's University, Kingston, Ontario, Canada, 2003.
[53] C.A. Mahieux, K.L. Reifsnider, S.W. Case, Property modeling across transition temperatures in PMC's: part I. Tensile properties, Appl Compos Mater 8 (2001) 217–234.
[54] A. Gibson, Y. Wu, J.T. Evans, A. Mouritz, Laminate theory analysis of composites under load in fire, J. Compos. Mater. 40 (2006) 639–658.